Available online at www.sciencedirect.com
SCIENCE DIRECT®
Polymer 44 (2003) 6989–6994
polymer
www.elsevier.com/locate/polymer

Synthesis of exfoliated poly(styrene-*co*-acrylonitrile) copolymer/silicate nanocomposite by emulsion polymerization; monomer composition effect on morphology

Yeong Suk Choi, Mingzhe Xu, In Jae Chung*

Department of Chemical and Biomolecular Engineering, Korea Advanced Institute of Science and Technology (KAIST), 373-1, Kusong-dong, Yusong-gu, Taejon 305-701, South Korea

Received 31 March 2003; received in revised form 3 July 2003; accepted 5 August 2003

Abstract

Two types of SAN/silicate nanocomposites were prepared to set up the relationship between the composition of monomers and the resultant morphology of the composites using a pristine sodium montmorillonite (Na-MMT). SAN I series were synthesized with acrylonitrile in initial stage and a mixture of styrene and acrylonitrile in increment stage. SAN II series were prepared with the mixture of styrene and acrylonitrile throughout polymerization. SAN I series showed exfoliated states but SAN II series exhibited intercalated states because SAN I series consisted of hydrophilic AN initially. The chemical affinity between monomer and silicate had a strong influence on the morphology of SAN/silicate nanocomposites. The exfoliated SAN I series had enhanced moduli and glass transition temperatures, T_g, compared to the intercalated SAN II series and pure SAN.

Keywords: Poly(styrene-*co*-acrylonitrile) copolymer; Silicate; Nanocomposites

1. Introduction

Nylon-6/silicate [1,2] nanocomposites by Toyota group opened a novel field of materials to researchers or engineers, because the composites exhibited balanced mechanical properties such as tensile strength and modulus. The composites attracted many researchers' attention to the development of polymer/silicate nanocomposites with excellent properties. From a morphological point of view, polymer/silicate nanocomposites were generally classified as two forms; intercalated and exfoliated. Exfoliated polymer/silicate nanocomposites were considered to have better mechanical properties than intercalated polymer/silicate nanocomposites due to uniform dispersion of silicate layers in polymer matrix. To prepare exfoliated polymer/silicate nanocomposites, various methods were developed: melt intercalation [3–5], in situ polymerization [2], curing systems [6], and sol–gel methods [7]. Unfortunately, most polymer/silicate nanocomposites showed intercalated morphology except few cases. For the preparation of polymer/silicate nanocomposites, researchers considered several points such as the surface character, regular structure of pristine silicates [8–10], and the compatibility between silicates and polymers. So a few organic modifiers [11–14] were adopted to modify silicate layers organophilic, but it needed additional process for modifications of silicates. One brilliant idea was to connect silicate layers and polymers covalently using modifiers containing reactive sites or anchoring initiators on the surface of silicates [15–17], but this method also included a step for the modification of pristine silicates. Recently, we prepared the exfoliated polymer/silicate nanocomposites through emulsion polymerizations without using any modifiers [24,25], and the nanocomposites had storage moduli enhanced over a large loading range of silicates. It can be explained that water, monomers, and reactive surfactants made the basal space of silicate wide before polymerizations, and then the silicate lost regularity and was exfoliated during the polymerization. This method will be applied to poly(styrene-*co*-acrylonitrile) copolymer (SAN) in this paper. The main focus of this paper is to synthesize

* Corresponding author. Tel.: +82-42-869-3916; fax: +82-42-869-3910.
E-mail address: chung@kaist.ac.kr (I.J. Chung).

0032-3861/$ - see front matter © 2003 Elsevier Ltd. All rights reserved.
doi:10.1016/j.polymer.2003.08.020

the exfoliated SAN/silicate nanocomposites. Up to now, several groups attempted to prepare SAN/silicate nanocomposites [18–22], but they obtained only the intercalated SAN/silicate nanocomposites. We will examine a method for preparation of exfoliated SAN/silicate nanocomposites, and explain why the silicate layers are exfoliated.

2. Experimental section

2.1. Materials

Styrene (ST), acrylonitrile (AN), and 2-acrylamido-2-methyl-1-propanesulfonic acid (AMPS) [23] were purchased from Aldrich and used as received. The silicate we used in this paper was sodium montmorillonite (Na-MMT) of Kunipia-F purchased from Kunimine Co. and the silicate had 119 mequiv./100 g of cation exchange capacity. Pristine silicate was dispersed in deionized water for 12 h at ambient temperature before polymerization. Potassium persulfate (KPS) of Junsei, a radical initiator, was recrystallized using deionized water. Tetrahydrofuran (THF) of HPLC solvent grade was used as received from Fluka for extraction. *N*,*N*-Dimethylformamide (DMF) of HPLC solvent grade, a good solvent for SAN, was used as received from Aldrich for polymer recovery in reverse ion exchange. Methyl alcohol (MeOH) of Fluka, a nonsolvent for PAN, was distilled at a normal pressure. Lithium chloride (Junsei) was recrystallized with THF.

2.2. Synthesis of SAN/silicate nanocomposites

Two types of poly(styrene-*co*-acrylonitrile) copolymer (SAN)/silicate nanocomposites were synthesized through a semi-batch emulsion polymerization to set up the relationship between the composition of monomers [26,27] charged in initial stages and the resultant morphology of the composites. For the synthesis of SAN I/silicate a designed amount of aqueous silicate dispersion, and a deionized water of 120 g were charged into a 1000 ml four-neck glass reactor fitted with a condenser, a rubber septum, a stirrer and a nitrogen inlet, and the reactor was stirred at 200 rpm under a nitrogen atmosphere at room temperature. 2-Acrylamido-2-methyl-1-propanesulfonic acid (AMPS) of 0.3 g, a reactive surfactant, acrylonitrile (AN) of 3 g, and aqueous initiator solution of 4 g (1 wt%) were charged into the reactor, and stirred for 30 min to make the mixture disperse uniformly under N_2 atmosphere. Temperature of the reactor was raised up to 75 °C to initiate the initial stage of polymerization and maintained for 30 min. After initial polymerization completed, 17 g of mixed monomer (ST/AN = 10 g/10 g) was fed continuously into the reactor with a syringe pump at a rate of 0.2 cc/min at the same temperature. After monomer feed was completed, the temperature of the reactor was increased to 90 °C and stirred for additional 3 h to further polymerization of residual monomers. Resultant nanocomposites were recovered by a freeze-drying method for 5 days and further dried at 50 °C for 50 h.

For SAN II/silicate nanocomposites, 5 g of mixed monomer (ST/AN = 10 g/10 g) was charged into the reactor instead of 3 g of AN used in the initial stage of SAN I/silicate nanocomposite. The initial polymerization was carried out for 1 h, and 15 g of the mixed monomer (ST/AN = 10 g/10 g) was charged at a rate of 0.2 cc/min in the incremental stage of polymerization. The other procedure was done in the same way as in SAN I series.

2.3. Polymer recovery

A small amount of the freeze-dried nanocomposite was extracted with DMF/LiCl solution (60 g/0.2 g = DMF/LiCl) under a nitrogen atmosphere at 80 °C for 5 days in a 500 ml three-neck reactor fitted with a condenser and a nitrogen inlet. The mixture was centrifuged at 6000 rpm for 30 min to separate polymers from the silicate cakes. The extract was filtered with a 0.45 μm membrane filter to remove silicates or unwanted particles and poured into MeOH (10–20 fold) to precipitate the polymers. The precipitated polymers were filtered and dried in a high vacuum at 50 °C for 50 h.

2.4. Measurements

Infrared spectra were recorded on a Bomem 102 FT-IR spectrometer with KBr pellets. A total of 40 scans taken at 4 cm^{-1} of resolutions were averaged. X-ray diffraction patterns were obtained by using Rigaku X-ray generator (Cu Kα with λ = 0.15406 nm) at room temperature with a scanning rate of 2°/min in a 2θ range of 1.2–10°. X-ray patterns for dried samples and for aqueous clay dispersions were obtained from the solid disc and the dispersed state, respectively.

Number average molecular weights were determined by using GPC. GPC analysis were performed at a flow rate of DMF 1.0 ml/min at 80 °C using a Polymer Laboratories 220 GPC system equipped with three styragel columns (500, two 10^6) and a RID detector after calibration with 10 polystyrene standards obtained from Easical Co.

tan δ and storage modulus (E') were obtained by a Rheometric Scientific DMTA4 with a dual cantilever from 30 to 180 °C with a heating rate of 5 °C/min under 0.04% of deformation at 1 Hz of frequency. Samples were molded in 12 × 25 × 1 mm^3 size at 140 °C for 3 min under 3000 psi of pressure. Glass transition temperatures, T_g, of the nanocomposites and pure polymer were determined from the maximum values in the tan δ vs temperature scan. The morphology of the nanocomposite was examined by a Philips CM-20 transmission electron microscope. The nanocomposite was sliced in 100 nm thickness and put on a carbon coated grid. The accelerating voltage of TEM was 160 kV.

Basal spaces of silicate dispersed in water with KPS, acrylonitrile, styrene, and AMPS were measured before the polymerization, because they would offer a lot of crucial information on exfoliation behavior of silicate during polymerization. AN, AMPS, and a mixture of acrylonitrile and AMPS were added into three beakers containing a clay dispersion and then water was added to make the concentration of ingredients equal to that of a nanocomposite containing 5 wt% of silicate in the initial stage. Styrene, KPS, and a mixture of styrene and AMPS were poured into beakers containing 3 wt% of silicate. The mixtures were stirred for 1 h to measure X-ray diffraction patterns.

3. Results

SAN I series have acrylonitrile in the initial stage and a mixture of styrene and acrylonitrile in incremental stage, and SAN II series have the mixture of styrene and AN throughout polymerization. T stands for pristine Na-MMT. Numbers next to T indicate the relative weight percentage of pristine silicate to the weight of total monomer. For example, SAN I T10% nanocomposite includes AMPS of 0.3 g, acrylonitrile of 3 g in the initial stage, mixed monomer of 17 g (ST/AN = 10 g/7 g) in the incremental stage, and 10 wt% of pristine Na-MMT.

Fig. 1 shows the FT-IR spectra of (a) pure polymer (SAN I T0%), and (b) nanocomposite (SAN I T10%). The FT-IR spectrum of SAN I T10% shows aromatic C–H stretching at around 3010–3100 cm^{-1}, aliphatic C–H stretching at around 2800–2993 cm^{-1}, C≡N stretching at 2243 cm^{-1}, and C–H bending at 1460 cm^{-1}, which are characteristic absorbance bands of poly(styrene-*co*-acrylonitrile) (SAN) copolymer. Absorbance bands at about 3627, 1043, and 620–513 cm^{-1} in Fig. 1(b), which are not present in the pure polymer, were assigned to OH stretching, Si–O stretching, Al–O stretching, and Si–O bending of pristine silicate in the composite. These bands indicate the presence of poly(styrene-*co*-acrylonitrile) copolymers (SAN) with silicate.

A small part of nanocomposite was extracted with

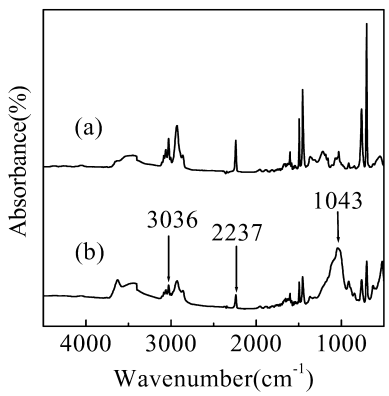

Fig. 1. FT-IR spectra of (a) SAN I T0% and (b) SAN I T10%.

THF to remove oligomers or water molecules which contribute to the expansion of interlayer space of the silicate. The extracted nanocomposite was dried under a high vacuum at 50 °C for 50 h and molded in a shape of a disk at 3000 psi of pressure. Fig. 2 shows X-ray diffraction patterns of SAN/silicate nanocomposites. In Fig. 2(a), SAN I series exhibit no peaks in the range of 1.2–10°. It indicates that SAN I series have an exfoliated morphology within 10 wt% of silicates loaded. While, SAN II series exhibit broad peaks in Fig. 2(b) indicating the intercalated morphology. A diffraction peak of SAN II T3% due to (001) planes of silicate occurs at 5.48°, and its *d* spacing is 1.61 nm. SAN II T5% shows the peak at 4.45° with a *d* spacing of 1.98 nm. The peak of SAN II T10% appears at 4.86°, and its *d* spacing is 1.81 nm. When acrylonitrile (AN) was added in the initial stage of polymerization, it enlarged the interlayer space of the silicate and made the silicate layers exfoliated in SAN I/silicate nanocomposites because AN had higher hydrophilicity and stronger interaction with the silicate layers than styrene (ST). This is why SAN I/silicate nanocomposites show the exfoliated structure. In order to prove this, X-ray patterns for aqueous dispersions of silicate with monomers, KPS, and AMPS were examined.

Fig. 3 shows interlayer space of silicates in water dispersion, which explains the state of silicate in the initial

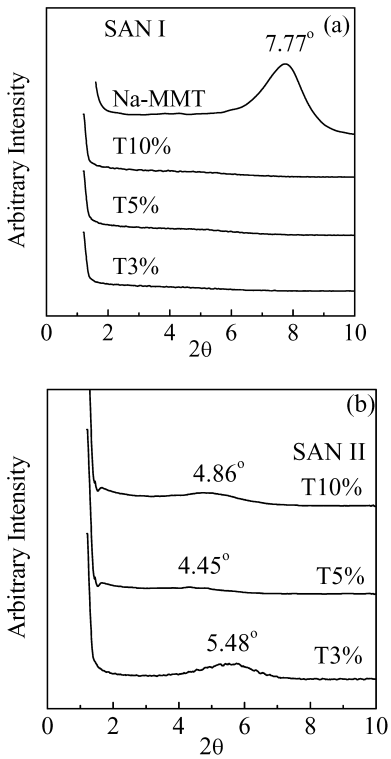

Fig. 2. X-ray diffraction patterns of SAN/silicate nanocomposites of (a) SAN I series and (b) SAN II series extracted using THF for 12 h with a Soxhlet extraction apparatus. Pristine silicate is given as a reference and measured based on a powder method.

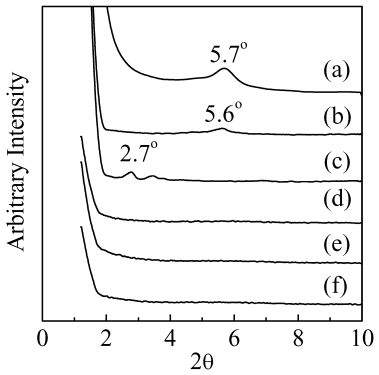

Fig. 3. X-ray diffraction patterns of water dispersions of pristine silicate under various conditions: (a) the dispersion of silicate in water, (b) with styrene, (c) with styrene and AMPS, (d) with KPS, (e) with AN, and (f) with AN and AMPS.

stage. Interlayer space of pristine silicate is enlarged with water, showing (001) plane diffraction at 5.7° (*d* spacing of silicate layers: 1.55 nm) in Fig. 3(a). The diffraction peak of aqueous dispersion of silicate containing ST shows (001) plane diffraction at 5.6° (1.58 nm), and the diffraction peak of aqueous dispersion of silicate with ST and AMPS show at 4.2° (2.1 nm). While, KPS (Fig. 3(d)), AN (Fig. 3(e)), and AMPS (Fig. 3(f)) also make the interlayer space of silicate further wide in the aqueous dispersion, showing no discernable diffraction patterns. These X-ray peaks indicate that AN has a higher interaction with silicate layers than ST, and the amount of AN in the interlayer space of silicate is higher than that of ST. It also means that as certain portions of the initiator, acrylonitrile, and AMPS are present in the interlayer space of the silicate, we can induce polymerization in the interlayer space easily. That leads the exfoliated state of the SAN I/silicate nanocomposites.

Fig. 4. TEM micrographs of SAN I T10%.

TEM is used to confirm the morphology of nanocomposites in Fig. 4, in which pristine silicate layers look like dark strips, and poly(styrene-*co*-acrylonitrile) copolymer appears as relatively bright domains. Delaminated layers of silicate in SAN I T10% are well distributed in entire SAN matrix, so the exfoliated morphology of SAN I/silicate nanocomposite is confirmed.

Table 1 shows the molecular weights of styrene-acrylonitrile (SAN) copolymer in the nanocomposites. The number-average molecular weights (M_n) of copolymers decrease as the content of silicate increases. It may be interpreted as follows: Because silicate absorbs monomers, initiators, and AMPS in the interlayer space of silicate, monomer-swollen silicate will be the polymerization site. As the amount of silicate increases, polymerization site will increase, and the molecular weight of SAN will decrease.

Fig. 5(a) exhibits the storage moduli, E', of SAN I series. At 40 °C, the storage moduli of the composites are 2.22×10^9 Pa for SAN I T0%, 2.56×10^9 Pa for SAN I T3%, 3.35×10^9 Pa for SAN I T5%, and 3.87×10^9 Pa for SAN I T10%. For SAN II series in Fig. 5(b), modulus of SAN II T0% is 2.09×10^9 Pa, SAN II T3% is 3.15×10^9 Pa, SAN II T5% is 3.25×10^9 Pa, and SAN II T10% is 3.44×10^9 Pa. SAN I series show enhanced moduli compared to SAN II series, because SAN I series, we think, have more the content of AN near silicate layers as well as higher molecular weights than SAN II series. The exfoliation of silicate layers in SAN I series also causes the enhancements.

Glass transition temperature, T_g, of each nanocomposite is obtained from the maximum temperature of tan δ in Fig. 6. SAN I T0% and SAN I T3% have the transitions at 134 °C, and SAN I T5% shows the transition at about 135 °C, but SAN I T10% shows the transition at 138 °C in Fig. 6(a). In Fig. 6(b), the transitions, T_g, of SAN II series appear at lower temperatures than the pure polymer. SAN II T0%, SAN II T3%, SAN II T5%, and SAN II T10% show the transitions at 134, 122, 132, and 126 °C, respectively. The decrease of glass transition temperatures for SAN II series may be related to molecular weight distribution of SAN matrix. A polymer with broad molecular weight

Table 1
Molecular weights of SAN recovered from SAN I and SAN II series nanocomposites

Samples	M_n	M_w	PDI
SAN I T0%	432,600	1,256,000	2.90
SAN I T3%	180,300	364,200	2.02
SAN I T5%	273,100	911,900	3.34
SAN I T10%	169,900	313,100	1.84
SAN II T0%	236,700	559,300	2.36
SAN II T3%	178,800	311,600	1.74
SAN II T5%	174,600	750,600	4.30
SAN II T10%	258,100	2,951,000	11.43

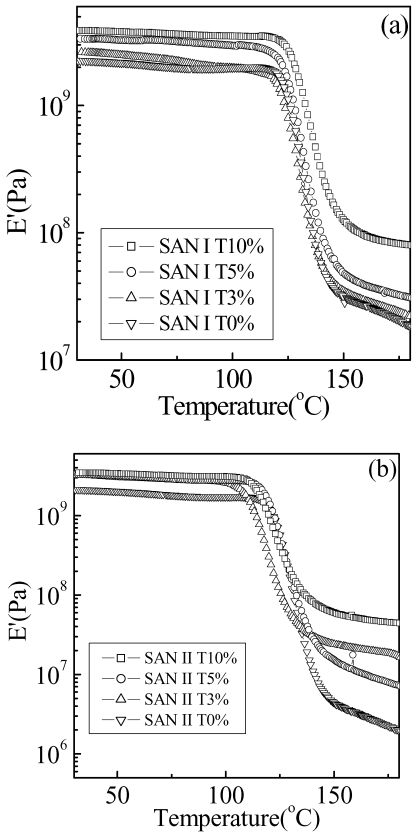

Fig. 5. Dependence of storage modulus of (a) SAN I series and (b) SAN II series on temperature with DMA.

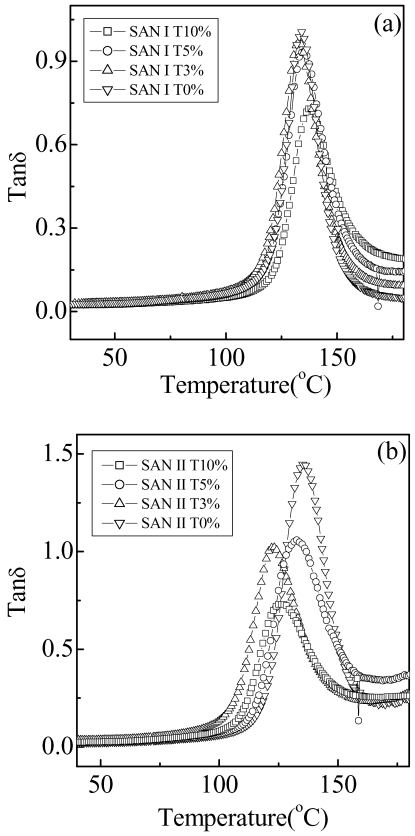

Fig. 6. tan δ of (a) SAN I series and (b) SAN II series obtained by using DMA.

distribution may contains low molecular weight portion, and the low molecular weight materials will drop the glass transition temperatures like plasticizers or lubricants [24]. SAN I series have higher glass transition temperatures than SAN II series because SAN I series have more acrylonitrile in silicate layers and the exfoliated structures.

4. Conclusion

We synthesized the exfoliated SAN/silicate nanocomposites and proved that the morphology of SAN/silicate nanocomposites was affected by the composition of monomers having different interactions with silicate layers. SAN I series containing acrylonitrile in the initial stage of polymerization exhibited the exfoliated states. While SAN II series consisted of ST and AN showed the intercalated states. Because SAN I series had higher content of strong negative and hydrophilic AN near silicate than SAN II series, the exfoliated structure in SAN I series were obtained. SAN I series had higher storage moduli than SAN II series. The glass transition temperature, T_g, for SAN I series increased with the content of silicate, but SAN II series had lower T_g than pure SAN.

Acknowledgements

Authors would like to express the sincere thanks to KOSEF (Korea Science and Engineering Foundation), CAFPoly (Center for Advanced Functional Polymers), and BK 21 program for their financial support.

References

[1] Kojima Y, Usuki A, Kawasumi M, Okada A, Kurauchi T, Kamigaito O. J Polym Sci, Part A: Polym Chem 1993;31:983.
[2] Kojima Y, Usuki A, Kawasumi M, Okada A, Kurauchi T, Kamigaito O. J Polym Sci, Part A: Polym Chem 1993;31:1755.
[3] Manias E, Touny A, Wu L, Strawhecker K, Lu B, Chung TC. Chem Mater 2001;13:3516.
[4] Ren J, Silva AS, Krishnamoorti R. Macromolecules 2000;33:3739.
[5] Gilman JW, Jackson CL, Morgan AB, Harris Jr R, Manias E, Giannelis EP, Wuthenow M, Hilton D, Philips SH. Chem Mater 2000; 12:1866.
[6] Byun HY, Choi MH, Chung IJ. Chem Mater 2001;13:4221.
[7] Templin M, Franck A, Chesne AD, Leist H, Zhang Y, Ulrich R, Schädler V, Wiesner U. Nature 1997;278:1795.
[8] Pinnavaia TJ. Science 1983;220:365.
[9] Tolbert SH, Firouzi A, Stucky GD, Chmelka BF. Nature 1997;278: 264.
[10] Kinrade SD, Nin JWD, Schach AS, Sloan TA, Wilson KL, Knight CTG. Science 1999;285:1542.
[11] Vaia RA, Teukosky RK, Giannelis EP. Chem Mater 1994;6:1017.

[12] Ginzburg VV, Balazs AC. Adv Mater 2000;12:1805.
[13] Balazs AC, Singh C, Zhulina E, Lyatskaya Y. Acc Chem Res 1999; 32:651.
[14] Beyer FL, Tan NCB, Dasgupta A, Galvin ME. Chem Mater 2002;14: 2983.
[15] Leu CM, Wu ZW, Wei KH. Chem Mater 2002;14:3016.
[16] Weimer MW, Chen H, Giannelis EP, Sogah DY. J Am Chem Soc 1999;121:1615.
[17] Bergman JS, Chen H, Giannelis EP, Thomas MG, Coates GW. Chem Commun 1999;2179.
[18] Kim JW, Choi HJ, Jhon MS. Macromol Symp 2000;155:229.
[19] Yoon JT, Jo WH, Lee MS, Ko MB. Polymer 2001;42:329.
[20] Kim JW, Noh MH, Choi HJ, Lee DC, Jhon MS. Polymer 2000;41: 1229.
[21] Noh MH, Lee DC. J Appl Polym Sci 1999;74:2811.
[22] Ko MB. Polym Bull 2000;45:183.
[23] Aota H, Akaki SI, Morishima Y, Kamachi M. Macromolecules 1997; 30:4090.
[24] Choi YS, Choi MH, Wang KH, Kim SO, Kim YK, Chung IJ. Macromolecules 2001;34:8978.
[25] Choi YS, Wang KH, Xu M, Chung IJ. Chem Mater 2002;14:2936.
[26] Okubo M, Lu Y. Colloid Polym Sci 1996;274:1020.
[27] Gan D, Lyon LA. J Am Chem Soc 2001;123:8203.